Anomalously fast convergence of India and Eurasia caused by double subduction

Oliver Jagoutz[1]*, Leigh Royden[1], Adam F. Holt[2] and Thorsten W. Becker[2]

Before its collision with Eurasia[1-5], the Indian Plate moved rapidly, at rates exceeding 140 mm yr^{-1} for a period of 20 million years[1,3-7]. This motion is 50 to 100% faster than the maximum sustained rate of convergence of the main tectonic plates today[8]. The cause of such high rates of convergence is unclear and not reproduced by numerical models[9,10]. Here we show that existing geological data[11,12] support the existence of two, almost parallel, northward dipping subduction zones between the Indian and Eurasian plates, during the Early Cretaceous period. We use a quantitative model to show that the combined pull of two subducting slabs can generate anomalously rapid convergence between India and Eurasia. Furthermore, in our simulations a reduction in length of the southern subduction system, from about 10,000 to 3,000 km between 90 and 80 million years ago, reduced the viscous pressure between the subducting slabs and created a threefold increase in plate convergence rate between 80 and 65 million years ago. Rapid convergence ended 50 million years ago, when the Indian Plate collided with the southern subduction system. Collision of India with Eurasia and the northern subduction system had little effect on plate convergence rates before 40 million years ago. We conclude that the number and geometry of subduction systems has a strong influence on plate migration rates.

The northward motion of India from the Early Cretaceous period to the Early Cenozoic era is related to the subduction of oceanic lithosphere north of India, which consumed the Neo-Tethys Ocean[13], and to seafloor spreading south of India, which created the Indian Ocean[14]. During the Cretaceous to Early Tertiary period, multiple subduction systems operated within the Neo-Tethys, including a north-dipping subduction boundary beneath the southern margin of Eurasia (for example, ref. 11) and, as proposed here, a second, intra-oceanic 'Trans-Tethyan' subduction system that extended from the eastern Mediterranean to Indonesia, and perhaps beyond (Fig. 1)[12].

The preserved geologic entities that make up this Cretaceous to Early Tertiary 'Trans-Tethyan subduction system' are, from west to east: the Antalya nappes and Cyprus ophiolite of southern Turkey[15]; the peri-Arabian ophiolites in the Middle East (labelled PA in Fig. 1) and the Semail ophiolite in Oman[15] (labelled Sm); ophiolitic and arc sequences of western Pakistan (Bela, Waziristan ophiolites[16]); the Kohistan–Ladakh Arc (labelled K) and associated ophiolites of the western Himalaya[17] (labelled X); supra-subduction ophiolites, forearc sequences and oceanic mélange sequences of the Tsangpo suture zone in the central and southern Himalaya[18,19]; ophiolitic and magmatic remnants in the Andaman Islands and Sumatra (Woyla Arc[12] (W); Fig. 1). By at least the mid-Cretaceous, this subduction boundary seems to have been everywhere north-dipping[12,15] (Fig. 2).

The existence of this Trans-Tethyan subduction system is consistent with the presence of two relict slabs below India[20]. At the longitude of the Himalaya, palaeomagnetic data show that in the Cretaceous, rocks of the Trans-Tethyan subduction system (Kohistan–Ladakh Arc and ophiolites of the Tsangpo suture zone) formed near the equator[18,21,22], whereas the magmatic rocks developed along the southern margin of Eurasia (Karakoram–Gangdese Arc, labelled Km, G and M in Fig. 1) formed at ~20°–25° N (ref. 23). This indicates that the two subduction systems were separated by an approximately 1,500–3,000 km wide oceanic plate, here called the Kshiroda Plate (Fig. 1).

Before the initiation of spreading in the Indian Ocean (~120–130 Myr ago (ref. 5)), a spreading ridge must have existed between India and Eurasia to accommodate subduction in the Neo-Tethys whereas little convergence occurred between the southern continents and Eurasia[5]. We place this ridge south of the Trans-Tethyan subduction system because spreading along its eastern extension is needed north of Australia to prevent its northward motion until the Woyla and Sumatra arcs become inactive at 90 Myr.

The timing of subduction along the Trans-Tethyan subduction system is crucial for understanding the convergence history of India and Eurasia. From the Semail ophiolite westwards, intra-oceanic subduction ended at ~90–80 Myr when the arc collided with the northern margin of Arabia[15] (Fig. 1). In Sumatra, intra-oceanic subduction ended at ~90 Myr, with northward obduction of the Woyla Arc onto continental crust[12]. Andean subduction in Sumatra also ended at about the same time[12].

In contrast, subduction along the central portion of the Trans-Tethyan subduction system continued along an approximately 3,000 km segment that formed the northern margin of the Indian Plate (Fig. 1)[17]. Evidence for continued subduction until ~50 Myr is well established in the western Himalaya[17]. New geochronological and isotopic data from the western Himalaya[17] show a ~50 Myr collision of the Indian subcontinent with the Kohistan–Ladakh Arc and a ~40 Myr collision of the amalgamated arc-continent with Eurasia. This collisional history is also consistent with palaeomagnetic data from the Kohistan–Ladakh Arc[18,21], and with the timing of two major tectonic events observed in the Indian Ocean[2].

In the central to eastern Himalaya, most of the rocks related to the Trans-Tethyan subduction system are missing, but sporadic remnants of this subduction system remain[19]. In particular, an intra-oceanic mélange sequence near Xigaze yields Palaeocene fossil ages that attest to intra-oceanic subduction into the Early Tertiary[18,24,25].

Figure 3 shows plate circuit data constraining the convergence history of India and Eurasia[3,4]. Because Eurasia and Antarctica

[1]Department of Earth, Atmospheric and Planetary Sciences, MIT, Cambridge, Massachusetts 01890, USA. [2]Department of Earth Sciences, University of Southern California, Los Angeles, California 90089, USA. *e-mail: jagoutz@mit.edu
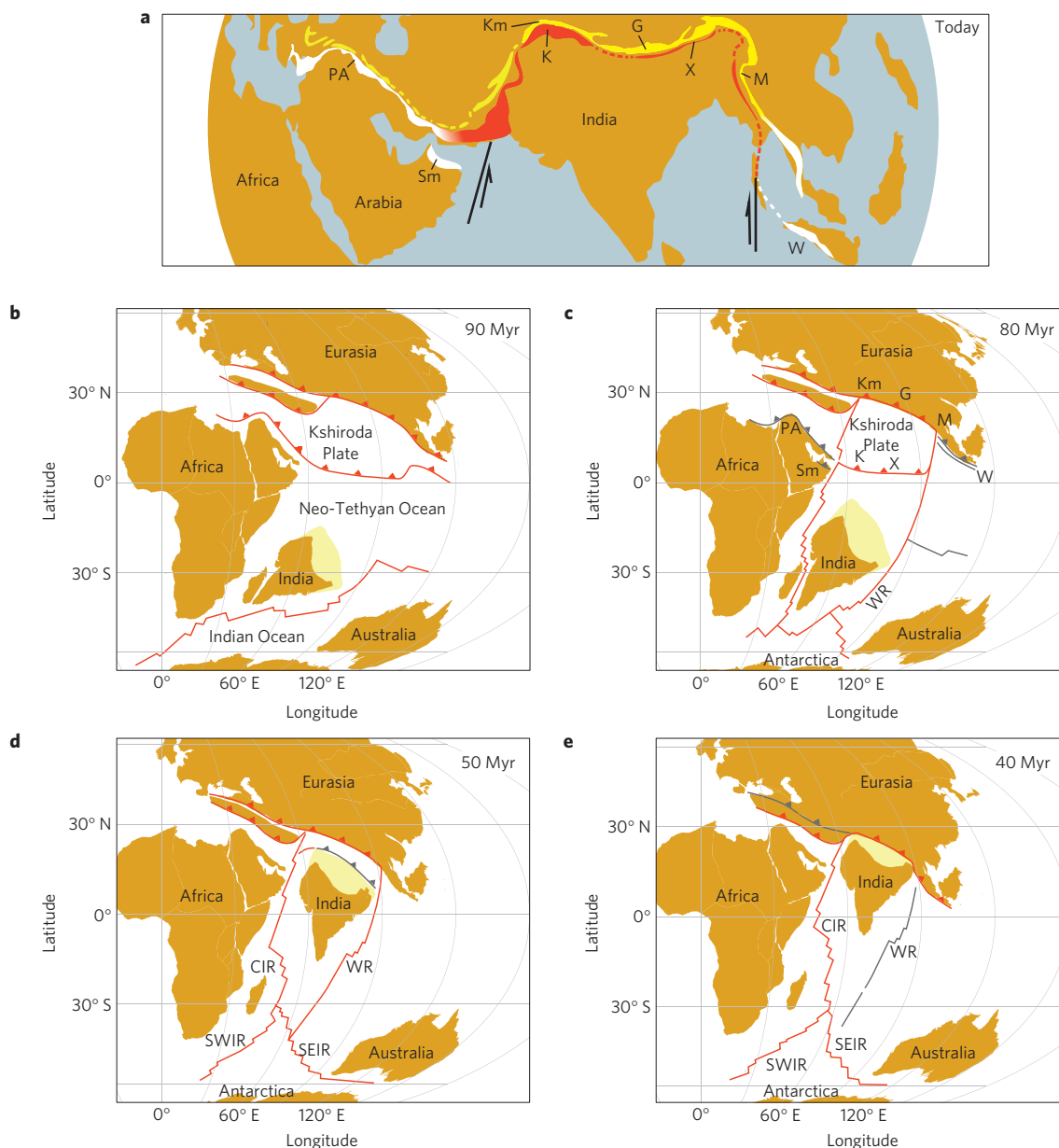
Figure 1 | Present day remnants of two subduction zones, and plate tectonic reconstructions for 90–40 Myr. a, Rocks related to subduction active after 80 Myr are red (Trans-Tethyan intra-oceanic system) and yellow (arc rocks of the Cretaceous subduction system of southern Eurasia). Rocks related to subduction that terminated before 80 Myr are white (both belts). Arrows show the sense of motion along the eastern and western margins of the Indian Plate after 80 Myr. **b–e**, Reconstructions of Neo-Tethyan plate boundaries; active boundaries shown in red, boundaries becoming extinct in grey. Red triangles indicate subduction, plain lines indicate spreading ridges and transform boundaries.

remained relatively stationary, rates of opening of the Indian Ocean are nearly identical to rates of India–Eurasia convergence, further constraining their pre-collisional history[1]. Before 80 Myr, convergence rates are not constrained by reliable sea floor magnetic anomalies, so we use palaeolatitude data to constrain convergence rates[23].

Figure 3 shows that, contemporaneous with the reduction in trench length of the Trans-Tethyan subduction system, India–Eurasia convergence rates began to increase rapidly. Simultaneously, the Wharton Ridge (labelled WR in Fig. 1) transform system initiated with a dominantly right-slip sense, forming the eastern boundary of the Indian Plate (Fig. 1) whereas spreading and left-slip on the Southwest Indian Ridge (SWIR) and Central Indian Ridge (CIR) accommodated divergence between India, Africa and Madagascar[5].

To investigate the effects of double subduction and the reduction in trench length of the subduction plate, we employ quantitative, three-dimensional models of coupled double subduction (that is, no spreading ridges present between the subduction systems, see Supplementary Fig. e1). Methods gives brief descriptions and benchmarking exercises for double subduction computed using two methods: an extension of the semi-analytic subduction technique described by ref. 26 (fast analytical subduction technique (FAST), described in detail in the Supplementary Information) and a fully numerical computation (an extension of CitcomCU; for example, ref. 27). The results of these techniques are very similar, indicating that the physics governing slab and plate motion is captured consistently. We choose to model the India–Eurasia convergence using FAST, which includes three-dimensional asthenospheric flow, topographic loading, slab bending and thrust interface coupling,
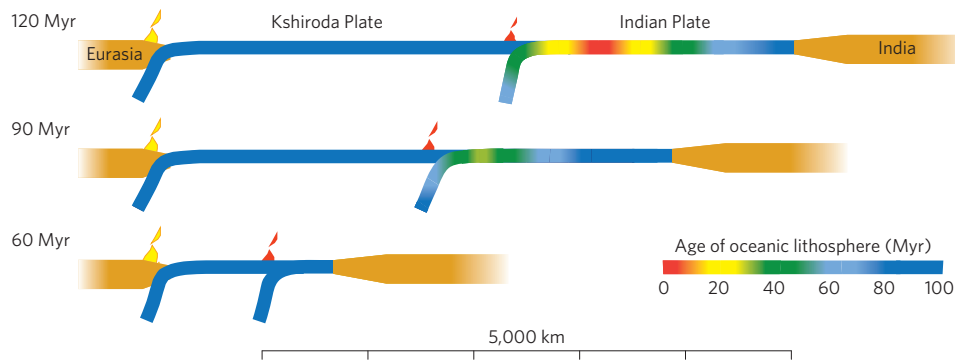
Figure 2 | Cross-sections of double subduction in the Tethys region. Slab geometries and distances between subduction systems and continents correspond to results of the model discussed in the text. The sea floor ages shown are those used as initial conditions in the model (at 120 Myr) and illustrate ageing of the oceanic lithosphere as derived from the model results. The yellow and red volcanoes indicate the volcanic arcs of the Southern Eurasian Margin and the Trans Tethyan subduction system, respectively.

and allows more efficient exploration of initial conditions and timing constraints over large space and time intervals. Details of the model parameters, initial conditions and timing constraints are given in Supplementary Table e1.

Rates of convergence across coupled double subduction systems are significantly faster than across single subduction systems because of slab pull by two slabs. However, convergence rates are strongly affected by trench length and by the distance separating the slabs; the latter decreases as subduction proceeds. As the distance between slabs decreases, asthenosphere must flow laterally out from between the slabs, creating a region of elevated viscous pressure between the slabs, and hindering convergence (Supplementary Fig. e1). Viscous pressure between slabs increases with decreasing slab separation and with increasing trench length because larger pressure gradients are needed to drive flow along narrower (distance between slabs) and longer (distance that scales with trench length) channels. Convergence rates are also affected by the size of the plates owing to viscous drag on the base of the plates.
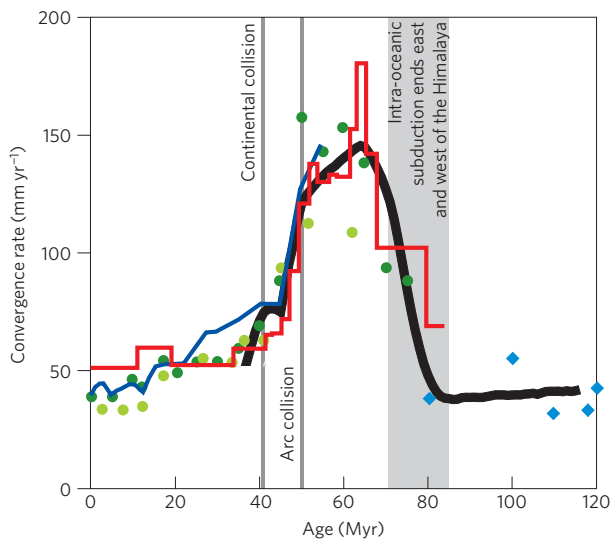

Figure 3 | Observed and model rates of India–Eurasia convergence.
Observations from plate circuit data (light green dots ref. 4; dark green dots ref. 3; blue line, ref. 4 as revised by ref. 3); Indian Ocean spreading (red line, refs 1,2); palaeolatitude data (blue diamonds, ref. 23). Black line shows computed convergence rate between India and Eurasia as described in the text. Grey shading shows timing of tectonic events in the quantitative model.

For the slab configurations in the Methods, the total plate length in each system is identical, but the convergence rate across the double subduction system is 150–170% faster than single subduction of a long plate beneath a short plate, and 220–250% faster than subduction of a short plate beneath a long plate, illustrating the importance of plate and slab geometry.

We model the pre-collisional convergence of India and Eurasia as coupled double subduction. The initial geometry is chosen to be consistent with the plate reconstructions shown in Fig. 1 and other constraints given in Supplementary Table e1. The initial model distance from the Eurasian margin to the incipient Indian Ocean is 9,300 km and the initial, trench-parallel width of the double subduction system is 10,000 km.

The initial conditions at 120 Myr were chosen to reproduce the observed timing of arc and continental collision[17] and palaeolatitude data that place the Kohistan Arc near the equator in the Cretaceous[21]. The initial conditions for the model presented here include a 3,150 km long (in N–S extent) Kshiroda Plate made up of old oceanic lithosphere. The oceanic portion of the northern Indian Plate is taken to be young oceanic lithosphere created by spreading at 40 mm yr^{-1} (Fig. 2), similar to the observed rate of spreading in the Indian Ocean from 120 to 90 Myr (ref. 23), and located 1,800 km north of the Indian continental margin.

We begin our model run at 120 Myr, following the slow initial rifting of India from Antarctica between 130 and 120 Myr (ref. 5). As constrained by the ages of ophiolite obduction east and west of the Indian Plate outlined above, we reduce the model trench length (in E–W extent) from 10,000 km to 3,000 km shortly after 90–80 Myr (refs 12,15; Supplementary Table e1). Although the time interval between ophiolite obduction, the end of subduction, and potential slab drop-off is uncertain, we estimate it to be ∼5–10 Myr. Therefore, we impose a tapered decrease in trench length between 85 and 70 Myr.

The model yields slow initial convergence at ∼40 mm yr^{-1} (Fig. 3), because viscous pressure is very high between slabs with a trench-parallel width of 10,000 km (Fig. 1) and young buoyant oceanic lithosphere, created at the extinct spreading ridge north of Greater India, is subducting beneath the Trans-Tethyan subduction system (Fig. 2). Model rates begin to increase at ∼80 Myr because trench-parallel narrowing of the Trans-Tethyan subduction system from 10,000 to 3,000 km reduces the viscous pressure between the slabs and the sea floor entering the Trans-Tethyan subduction system is ageing and becoming more negatively buoyant. The former effect dominates, producing more than three-quarters of the rate increase at 75–70 Myr.

Model rates peak at 146 mm yr^{-1} at ∼65 Myr, after which no further increase in (negative) slab buoyancy occurs. After 65 Myr,

the viscous pressure between slab increases again owing to decreasing separation of the slabs, which slows convergence slightly, even prior to collision. A marked slowing of convergence in the model results from the collision of India with the Trans-Tethyan subduction system, triggered by the partial subduction of buoyant continental crust. The collision of the amalgamated arc-continent with Eurasia at 40 Myr produces a less marked slowing of convergence. (We do not model post-collisional convergence because subduction along the northern margin of the combined Indo-Australian Plate has a more complex geometry than that used here.)

Our model reproduces the magnitude and temporal variation of the observed convergence rates (Fig. 3). In particular, we show that the threefold increase in India–Eurasia convergence rates between 80 and 65 Myr can be causally linked to the observed reduction in trench length of the Trans-Tethyan subduction zone, whereas the twofold slowing of convergence at ~50 Myr can be attributed to collision of India with the Trans-Tethyan subduction system.

Several studies have explored whether formation of the Reunion plume triggered anomalously rapid convergence of India and Eurasia (for example, ref. 1). Our modelling, in agreement with refs 10,29, suggests that the influence of the Reunion plume is limited, perhaps to the short time interval around ~66 Myr when spreading rates in the Indian Ocean reached ~180 mm yr^{-1}.

In conclusion, we propose that the subduction boundary beneath the southern margin of Eurasia and the Cretaceous to Early Tertiary intra-oceanic 'Trans-Tethyan' subduction system formed a coupled double subduction system located in the northern and central Neo-Tethys and caused anomalously fast motion of the Indian Plate. Quantitative modelling indicates that the observed geometry and timing of subduction along this double plate boundary system can account for almost all features of the pre-collisional convergence history of India and Eurasia.

Methods

Methods and any associated references are available in the online version of the paper.

References

1. Cande, S. C. & Stegman, D. R. Indian and African plate motions driven by the push force of the Reunion plume head. *Nature* **475,** 47–52 (2011).
2. Cande, S. C., Patriat, P. & Dyment, J. Motion between the Indian, Antarctic and African plates in the early Cenozoic. *Geophys. J. Int.* **183,** 127–149 (2010).
3. Copley, A., Avouac, J. P. & Royer, J. Y. India–Asia collision and the Cenozoic slowdown of the Indian Plate: Implications for the forces driving plate motions. *J. Geophys. Res.* **115,** B03410 (2010).
4. Molnar, P. & Stock, J. M. Slowing of India's convergence with Eurasia since 20 Ma and its implications for Tibetan mantle dynamics. *Tectonics* **28,** TC3001 (2009).
5. Besse, J. & Courtillot, V. Paleogeographic maps of the continents bordering the Indian Ocean since the Early Jurassic. *J. Geophys. Res.* **93,** 11791–11808 (1988).
6. Patriat, P. & Achache, J. India–Eurasia collision chronology has implications for crustal shortening and driving mechanism of plates. *Nature* **311,** 615–621 (1984).
7. White, L. T. & Lister, G. S. The collision of India with Asia. *J. Geodynam.* **56–57,** 7–17 (2012).
8. Goes, S., Capitanio, F. A. & Morra, G. Evidence of lower-mantle slab penetration phases in plate motions. *Nature* **451,** 981–984 (2008).
9. Capitanio, F., Morra, G., Goes, S., Weinberg, R. & Moresi, L. India–Asia convergence driven by the subduction of the Greater Indian continent. *Nature Geosci.* **3,** 136–139 (2010).
10. van Hinsbergen, D. J., Steinberger, B., Doubrovine, P. V. & Gassmöller, R. Acceleration and deceleration of India–Asia convergence since the Cretaceous: Roles of mantle plumes and continental collision. *J. Geophys. Res.* **116,** B06101 (2011).
11. Yin, A. & Harrison, T. M. Geologic evolution of the Himalayan–Tibetan orogen. *Annu. Rev. Earth Planet. Sci.* **28,** 211–280 (2000).
12. Hall, R. Late Jurassic–Cenozoic reconstructions of the Indonesian region and the Indian Ocean. *Tectonophysics* **570,** 1–41 (2012).
13. Sengor, A. M. C. & Natal'in, B. A. in *The Tectonic Evolution of Asia* (eds Yin, A. & Harrison, M.) 486–640 (Cambridge Univ. Press, 1996).
14. McKenzie, D. & Sclater, J. G. The evolution of the Indian Ocean since the Late Cretaceous. *Geophys. J. R. Astron. Soc.* **24,** 437–528 (1971).
15. Şengör, A. M. C. & Stock, J. The Ayyubid Orogen: An ophiolite obduction-driven orogen in the Late Cretaceous of the Neo-Tethyan South Margin. *Geosci. Can.* **41,** 225–254 (2014).
16. Gnos, E., Immenhauser, A. & Peters, T. Late Cretaceous/early Tertiary convergence between the Indian and Arabian plates recorded in ophiolites and related sediments. *Tectonophysics* **271,** 1–19 (1997).
17. Bouilhol, P., Jagoutz, O., Hanchar, J. & Dudas, F. Dating the India–Eurasia collision through arc magmatic records. *Earth Planet. Sci. Lett.* **366,** 163–175 (2013).
18. Aitchison, J. C. *et al.* Remnants of a Cretaceous intra-oceanic subduction system within the Yarlung-Zangbo suture (southern Tibet). *Earth Planet. Sci. Lett.* **183,** 231–244 (2000).
19. Hébert, R. *et al.* The Indus–Yarlung Zangbo ophiolites from Nanga Parbat to Namche Barwa syntaxes, southern Tibet: First synthesis of petrology, geochemistry, and geochronology with incidences on geodynamic reconstructions of Neo-Tethys. *Gondwana Res.* **22,** 377–397 (2012).
20. Van der Voo, R., Spakman, W. & Bijwaard, H. Tethyan subducted slabs under India. *Earth Planet. Sci. Lett.* **171,** 7–20 (1999).
21. Zaman, H. & Torii, M. Palaeomagnetic study of Cretaceous red beds from the eastern Hindukush ranges, northern Pakistan; palaeoreconstruction of the Kohistan–Karakoram composite unit before the India–Asia collision. *Geophys. J. Int.* **136,** 719–738 (1999).
22. Khan, S. D. *et al.* Did the Kohistan–Ladakh island arc collide first with India? *Geol. Soc. Am. Bull.* **121,** 366–384 (2009).
23. van Hinsbergen, D. J. *et al.* Greater India Basin hypothesis and a two-stage Cenozoic collision between India and Asia. *Proc. Natl Acad. Sci. USA* **109,** 7659–7664 (2012).
24. Burg, J. & Chen, G. Tectonics and structural zonation of southern Tibet, China. *Nature* **311,** 219–223 (1984).
25. Aitchison, J. C., Ali, J. R. & Davis, A. M. When and where did India and Asia collide? *J. Geophys. Res.* **112,** B05423 (2007).
26. Royden, L. H. & Husson, L. Trench motion, slab geometry and viscous stresses in subduction systems. *Geophys. J. Int.* **167,** 881–905 (2006).
27. Zhong, S. Constraints on thermochemical convection of the mantle from plume heat flux, plume excess temperature, and upper mantle temperature. *J. Geophys. Res.* **111,** B04409 (2006).
28. Boyden, J. A. *et al.* in *Geoinformatics: Cyberinfrastructure for the Solid Earth Sciences* (eds Keller, G. R. & Baru, C.) 95–114 (Cambridge Univ. Press, 2011).
29. Muller, R. D. Earth science: Plate motion and mantle plumes. *Nature* **475,** 40–41 (2011).
30. Morgan, W. J. & Morgan, J. P. Plate velocities in the hotspot reference frame. *Geol. Soc. Am. Spec. Pap.* **430,** 65–78 (2007).

Author contributions

O.J. and L.R. designed the project. L.R. and O.J. compiled the geology. L.R., A.F.H. and T.W.B. conducted the modelling. All authors contributed to analysing the results and writing the paper.

Additional information

Supplementary information is available in the online version of the paper. Reprints and permissions information is available online at www.nature.com/reprints. Correspondence and requests for materials should be addressed to O.J.

Competing financial interests

The authors declare no competing financial interests.

Methods

We use a semi-analytical, 'fast analytical subduction technique' (FAST) to calculate how the geometry of slabs evolves over time and how the induced stresses drive the plates. This updated version of the method in ref. 26 includes a more extensive treatment of large-scale flow of a Newtonian viscous asthenosphere.

At each time step, FAST progresses via several computations. We begin with the velocities of the plates, the geometries of the slabs, and the velocity of each point along the slabs as determined from the previous time step. From these, we derive the large-scale (regional) flow of the asthenosphere by treating the slabs as vertical boundaries using a Hele-Shaw approximation for viscous flow (Supplementary Fig. e1). The vertically averaged velocity $\overline{V}$, the dynamic pressure, P, and the velocity of the overlying plates, v_p, are related by:

$$\overline{V} = -\nabla P \left(\frac{h^2}{12\mu} \right) + \frac{v_p}{2} \qquad \nabla^2 P \left(\frac{h^2}{6\mu} \right) = \nabla \cdot v_p$$

where h is asthenosphere thickness and μ is viscosity. We solve for P such that it satisfies the left-hand equation on the slab surfaces (for $\overline{V}$ equals the horizontal slab velocity), and the right-hand equation elsewhere.

We then adjust the velocities of all foreland plates (that is, red and green plates in Supplementary Fig. e1), the applied topographic loads, and the coefficient of friction so as to maintain a zero net torque on each plate and to maintain the desired plate geometry (that is, upper plate fixed, and so on). Using an updated version of the approximation for viscous wedge flow by ref. 26, we compute flow in the asthenospheric wedges above and below the slabs. This solution is embedded within the solution for large-scale viscous flow such that the viscous pressure at the open ends of the asthenospheric wedges (Supplementary Fig. e2) is equal to that calculated at the same location in the large-scale flow field. Last, we derive the new slab geometry by solving the fourth-order ordinary differential equation for bending of a thin viscous sheet subject to the various sources of stress that act on the slabs. The slab geometries are then advected for the next time step.

For calibration, we applied FAST to the Pacific and Nazca plates, taking plate velocities in a hotspot reference frame from ref. 30. We approximated the Pacific Plate as a rectangle 6,000 km (trench length) by 8,000 km, with buoyancy equivalent to 6 km water depth, subducted beneath a fixed Eurasian Plate[30]. With all other parameters determined as in the main text, this yields a model Pacific Plate velocity of 72 mm yr^{-1} west, comparing favourably with observed velocities that vary from 60 mm yr^{-1} at the northern end of the Kuril Trench[30] to 90 mm yr^{-1}

near the southern end of the Marianna Trench[30]. We likewise approximated the Nazca Plate as a rectangle 4,000 km (trench length) by 3,000 km, with buoyancy equivalent to 5.5 km water depth, subducted beneath a South American Plate constrained to move west at 20 mm yr^{-1} (ref. 30). This yields a model Nazca Plate velocity of 56 mm yr^{-1} east, in good agreement with the observed motion of the Nazca Plate at 60 mm yr^{-1} (ref. 30).

We compared FAST against the fully numerical code CitcomCU[27]. Subduction in CitcomCU is modelled in a box with a dimensional height of 660 km, length of 5,280 km, and width of 5,280 km. The plates have an initial uniform thickness of 80 km and uniform temperature of 273 K. The initial negative buoyancy of the lithosphere is equivalent to an initial water depth of 5.5 km, with viscosities and lithospheric thicknesses as per Supplementary Table e1. Subduction is initiated with an asymmetric lithospheric geometry in the trench region to 150 km depth. A 15-km-thick crustal layer is inserted at the top of the subducting plate, with a viscosity half that of the asthenosphere and the same density as the mantle lithosphere. All boundaries are free slip.

Plate thickness, buoyancy, viscosity and the density of the mantle and asthenosphere were identical in CitcomCU and FAST. Important differences include the normal and shear stresses at the plate interface (FAST uses a frictional stress criterion whereas CitcomCU uses a weak viscous interface) and the occurrence of down-dip plate stretching in CitcomCU but not in FAST.

We analysed a coupled double subduction system (see Supplementary Fig. e1), where all plates are 1,320 km long, and single subduction in two scenarios: a short plate (1,320 km) subducting beneath a long plate (2,640 km) and a long plate (2,640 km) subducting beneath a short plate (1,320 km). All trench lengths were 2,000 km. The agreement between models is very good (Supplementary Fig. e4), most importantly after ∼6 Myr. when the slabs reach the base of the upper mantle. In this double subduction case there is no slowing of convergence with decreasing slab separation because trench lengths are short and the effect of decreasing plate length, which reduces mantle drag on the incoming plate, outweighs the effect of decreasing slab separation.